THE PROTEIN SOCIETY

Clostridium perfringens epsilon toxin H149A mutant as a platform for receptor binding studies

Monika Bokori-Brown,[1]* Maria C. Kokkinidou,[2] Christos G. Savva,[2] Sérgio P. Fernandes da Costa,[1] Claire E. Naylor,[2] Ambrose R. Cole,[2] David S. Moss,[2] Ajit K. Basak,[2] and Richard W. Titball[1]

[1]Biosciences, College of Life and Environmental Sciences, University of Exeter, Exeter EX4 4QD, United Kingdom
[2]Department of Biological Sciences, Institute of Structural and Molecular Biology, Birkbeck College, London WC1E 7HX, United Kingdom

Received 29 January 2012; Accepted 8 March 2013
DOI: 10.1002/pro.2250
Published online 18 March 2013 proteinscience.org

Abstract: *Clostridium perfringens* epsilon toxin (Etx) is a pore-forming toxin responsible for a severe and rapidly fatal enterotoxemia of ruminants. The toxin is classified as a category B bioterrorism agent by the U.S. Government Centres for Disease Control and Prevention (CDC), making work with recombinant toxin difficult. To reduce the hazard posed by work with recombinant Etx, we have used a variant of Etx that contains a H149A mutation (Etx-H149A), previously reported to have reduced, but not abolished, toxicity. The three-dimensional structure of H149A prototoxin shows that the H149A mutation in domain III does not affect organisation of the putative receptor binding loops in domain I of the toxin. Surface exposed tyrosine residues in domain I of Etx-H149A (Y16, Y20, Y29, Y30, Y36 and Y196) were mutated to alanine and mutants Y30A and Y196A showed significantly reduced binding to MDCK.2 cells relative to Etx-H149A that correlated with their reduced cytotoxic activity. Thus, our study confirms the role of surface exposed tyrosine residues in domain I of Etx in binding to MDCK cells and the suitability of Etx-H149A for further receptor binding studies. In contrast, binding of all of the tyrosine mutants to ACHN cells was similar to that of Etx-H149A, suggesting that Etx can recognise different cell surface receptors. In support of this, the crystal structure of Etx-H149A identified a glycan (β-octyl-glucoside) binding site in domain III of Etx-H149A, which may be a second receptor binding site. These findings have important implications for developing strategies designed to neutralise toxin activity.

Keywords: *Clostridium perfringens*; epsilon toxin; enterotoxemia; glycan binding; pore-forming toxin

Introduction

Epsilon toxin (Etx) is a pore-forming toxin and is produced by *Clostridium perfringens* strains belonging to toxinotypes B and D.[1] These strains are responsible for enterotoxemia, which affects mainly sheep but also occurs in goats and cattle, and results in heavy economic losses.[2,3] The disease is also known as overeating disease as it is often triggered by feeding on carbohydrate-rich food, leading to disruption of the microbial balance in the intestine and consequent proliferation of *C. perfringens* and overproduction of Etx.[4]

By an unknown mechanism, Etx crosses the gut wall, enters into the bloodstream and is disseminated to several organs, in particular to the kidneys

Grant sponsor: Wellcome Trust; Grant number: WT089618MA; Grant sponsor: European Union Marie Curie Network; Grant number: 237942.

*Correspondence to: Monika Bokori-Brown, College of Life and Environmental Sciences, Geoffrey Pope Building, University of Exeter, Stocker Road, Exeter EX4 4QD, United Kingdom. E-mail: m.bokori-brown @exeter.ac.uk

and the brain, where intoxication results in fluid accumulation due to increased permeability of blood vessels.[4] There is also evidence that Etx acts directly on the brain,[5–7] targeting glutamatergic neurons[8] and stimulating glutamate release. This may explain some of the neurological symptoms often associated with the disease in sheep, such as loss of coordination and seizures.[3,9,10]

Etx is secreted by *C. perfringens* as a prototoxin (P-Etx), which consists of 296 amino acids with a molecular weight of 32,981 Da.[11] The prototoxin is activated, with carboxy-terminal and amino-terminal peptides removed, by proteolytic cleavage in the gut, either by digestive proteases of the host, such as trypsin and chymotrypsin,[12] or by λ-protease produced by *C. perfringens*.[13,14]

The crystal structure of P-Etx has been determined[15] and reveals mainly β-sheets, which are organized into three functional domains. Domain I at the N-terminus contains the suggested receptor interaction region,[15,16] domain II contains an amphipathic β-hairpin, which is predicted to play a role in membrane insertion, and domain III at the C-terminus contains the C-terminal peptide, which has to be removed for activation.

The mechanism of pore formation by Etx is not well understood and the current pore formation model is based on studies of other β-pore-forming toxins (β-PFTs), such as aerolysin from *Aeromonas hydrophila*.[17] Like aerolysin, Etx binds to detergent-resistant microdomains (DRMs) of lipid rafts.[18–20] Both P-Etx and Etx can accumulate within DRMs but only activated toxin can oligomerize and form a heptameric complex. Heptameric complexes of Etx have been identified in rat synaptosomal, MDCK and $mpkCCD_{cl4}$ cell membranes.[21–23] The final step of pore formation might involve unfolding of the amphipathic β-hairpin in domain II and subsequent insertion of the toxin into the membrane, usually leading to rapid cell death.

Etx is unique among β-PFTs as it shows high cell specificity and potency. Relatively few cell lines are susceptible to the toxin and most *in vitro* studies on Etx have been carried out using the highly susceptible Madin–Darby Canine Kidney (MDCK) cell line.[24,25] Other toxin-sensitive cell lines include the mouse kidney cell line $mpkCCD_{cl4}$[23] and the recently identified human renal adenocarcinoma cell line ACHN.[26] Because of its high potency, and the potential to use Etx as a bioterrorist weapon, the toxin is classified as a category B bioterrorism agent by the U.S. Government Centres for Disease Control and Prevention.[27]

In view of the high potency of Etx, the aim of this study was to identify a platform that provided a reduction in the hazard associated with the genetic manipulation of recombinant *C. perfringens* epsilon toxin in *Escherichia coli* whilst allowing receptor binding studies. For this platform we selected the H149A variant of Etx (numbering corresponds to prototoxin without the 13 amino acids N-terminal peptide), which reduces toxicity sixfold in MDCK cells and 67-fold in mice.[28] This study has confirmed the role of tyrosine residues in domain I of Etx in binding to MDCK cells and has also revealed that additional receptor binding regions appear to play a role in toxicity of Etx.

Results

Mutation H149A does not affect P-Etx structure

To determine the effect of the H149A mutation on the tertiary structure of P-Etx, we crystallized recombinant P-Etx-H149A. Initial trials resulted in crystals, which grew in the presence of 0.85 to 1.0 *M* ammonium dihydrogen phosphate and diffracted to ~3 Å. However, the crystals were twinned with >45% twin fractions. In an attempt to reduce the degree of twinning, various additives were included in the crystallization conditions. One of the additives, β-octyl-glucoside (β-OG), resulted in crystals with lower twin fractions, and which diffracted to 2.4 Å. They belonged to the P3 spacegroup with unit cell dimensions of $a = 123.70$ Å, $b = 123.70$ Å, $c = 127.31$ Å, and $\alpha = \beta = 90^\circ$, $\gamma = 120^\circ$. The asymmetric unit (ASU) contained four P-Etx-H149A molecules, four β-OG molecules and four ordered phosphates. Due to the higher resolution of the P-Etx-H149A data compared with the original wild-type structure (PDB ID: 1UYJ, 2.6 Å) we detected a +1 residue register error in the wild-type structure from Ser3 to Gly14 (corresponds to Ser16 to Gly27 in PDB ID: 1UYJ).

Each β-OG molecule is accommodated in a cleft formed between two β-sheets in domain III of P-Etx-H149A and interacts through hydrogen bonds to Etx [Fig. 1(A), lower inset]. Specifically, the glucose moiety of β-OG forms hydrogen bonds via O5 to Thr93 main chain N and through O2 to Val72 mainchain O. In addition, in chains A and B, the O3 of β-OG forms a hydrogen bond to OE1 of Glu61 in the neighboring asymmetric unit. The alkyl chain of β-OG is in close proximity to Phe92 in all four Etx molecules. The four phosphate molecules also form hydrogen bonds to Etx through OD1 and OD2 of Asp48, OG of Ser188, and NE2 of Gln85 from the neighboring ASU. Moreover, strong positive density (>3 σ) in the Fo-Fc map could be seen near Y29 in all four chains in the ASU, and although the size of this density suggests additional bound β-OG molecules we could not place β-OG with certainty (data not shown).

The P-Etx-H149A structure closely resembles the wild-type structure with a Cα-Cα root mean square deviation (RMSD) of 0.95 Å [Fig. 1(B)]. Small main chain deviations occur in domains I, II and III compared to the wild-type structure. In domain I, at

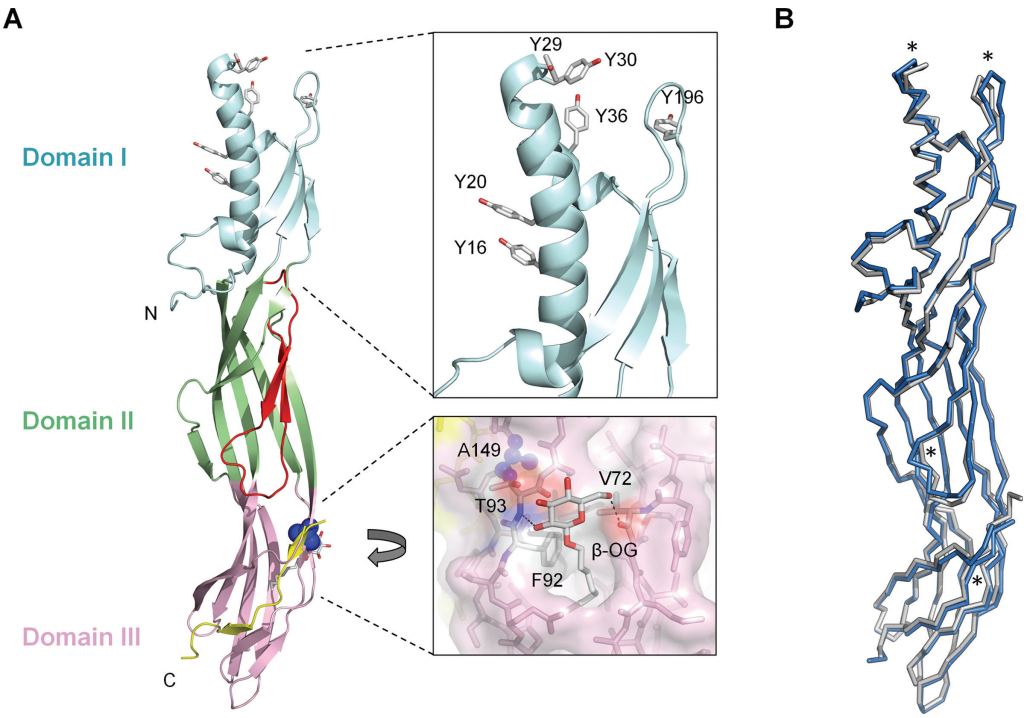

Figure 1. Structure of *C. perfringens* epsilon prototoxin P-Etx-H149A. (A) Cartoon representation of the prototoxin colored according to domain. The likely membrane-inserting β-hairpin is colored red. The C-terminal peptide is colored in yellow and situated near the pink oligomerization domain. Top inset shows the receptor binding region and the positions of the mutated tyrosines. The lower inset shows the location of A149 (blue spheres), the bound β-OG ligand and interacting residues. Amino acid numbering corresponds to prototoxin without the 13 amino acids N-terminal peptide sequence. (B) Superposition of wild-type prototoxin (PDB ID: 1UYJ, grey) with P-Etx-H149A (blue). Asterisks indicate the areas of highest RMS Cα-Cα deviation.

the end of the first α-helix near Y29, the Cα positions are shifted by 2.20 Å in respect to the wild-type structure. This may be due to the influence by putative β-OG molecules in this region as mentioned above. In addition, a loop between Ser195 and P200 is shifted by up to 2.58 Å away from the core of the molecule. In domain II, the membrane-inserting β-hairpin is shifted by up to 2.84 Å near Phe135. Finally, in domain III, the β-strand from V70 to N79 is displaced outwards by up to 2.05 Å in order to accommodate the β-OG molecule [Fig. 1(A), lower inset]. Overall, the H149A mutation does not have an effect on the prototoxin tertiary structure and does not induce any significant conformational changes in the suggested receptor binding loops in domain I. Collection and refinement statistics for the crystals are listed in Table I, and coordinates and structure factors have been deposited with the Protein Data Bank (PDB ID: 3ZJX).

Tyrosine mutants in H149A background mimic the binding of tyrosine mutants in wild-type background

Surface exposed tyrosine residues in domain I of Etx have recently been reported to play a role in binding to MDCK cells.[16] To evaluate the suitability of P-

Table I. *X-Ray Data Collection and Refinement Statistics*

	P-Etx-H149A
Data collection	
Space group	*P3*
Cell dimensions	
a, *b*, *c* (Å)	123.70, 123.70, 127.31
α,β,γ (°)	90, 90, 120
Resolution (Å)	21.56–2.40 (2.49–2.40)[a]
R_{merge}	0.061 (0.435)
$I/\sigma I$	12.3 (1.2)
Completeness (%)	100.0 (99.9)
Redundancy	3.70 (2.25)
Refinement	
Resolution (Å)	21.56–2.4
No. reflections	85,072
R_{work}/R_{free} (%)	24.6–27.5
No. atoms	
Protein	8448
Ligand/ion	100
Water	459
B-factors (Å^2)	
Protein	54.5
Ligand	48.2
Water	47.0
RMS deviations	
Bond lengths (Å)	0.01
Bond angles (°)	1.33

[a] Values in parentheses are for highest-resolution shell.

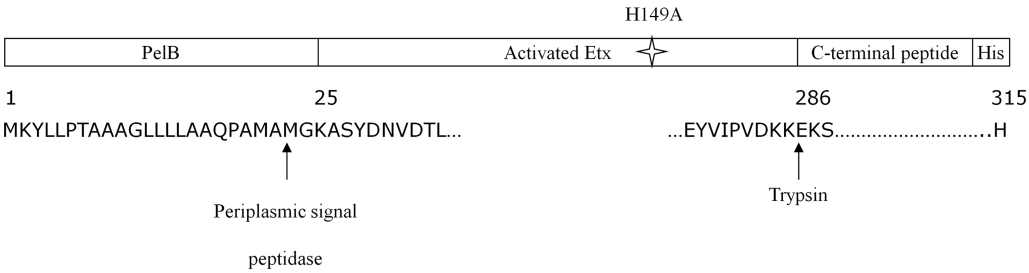

Figure 2. Schematic representation of recombinant *C. perfringens* epsilon prototoxin P-Etx-H149A. The amino acid sequences around the processing sites are shown. Amino acid numbering for H149A corresponds to prototoxin without the 13 amino acids N-terminal peptide sequence.

Etx-H149A for receptor binding studies, we selected six surface exposed tyrosine residues (Y16, Y20, Y29, Y30, Y36, and Y196) in domain I for site-directed mutagenesis and replaced each one with alanine [Fig. 1(A), top inset] to delete the side chain completely, and thus to allow a definitive determination of whether the side chain contributed to binding in any way.

Recombinant P-Etx-H149A (Fig. 2) and its derivatives were expressed and purified as described in Materials and Methods. All tyrosine mutants showed similar purification [Fig. 3(A)] and trypsin digestion [Fig. 3(B)] profiles to Etx-H149A, indicating that tyrosine mutations do not affect the folding of the toxin. Purified recombinant P-Etx-H149A and its derivatives have an apparent molecular weight of ~37 kDa as detected by SDS-PAGE [Fig. 3(A)]. Thermal stability assay[29] revealed that the melting temperature (T_m) of the tyrosine mutants was similar to that of P-Etx-H149A [Fig. 3(C)], providing further evidence that the tyrosine mutants are folded correctly.

On-Cell Western assays were used to evaluate the effect of the tyrosine mutations on the binding of P-Etx-H149A to MDCK.2 cells. The binding activity of each tyrosine mutant was expressed as the fold-change in fluorescence intensity relative to P-Etx-H149A (Fig. 4). Mutants Y30A and Y196A showed significant reduction in binding activity relative to P-Etx-H149A (20-fold and 6-fold decrease in fluorescent intensity, respectively).

Reduced binding of tyrosine mutants to MDCK.2 cells correlates with their reduced cytotoxicity

Next, we evaluated the effect of the tyrosine mutations on the cytotoxic activity of trypsin-activated Etx-H149A towards MDCK.2 cells by measuring the amount of lactate dehydrogenase (LDH) released from the cytosol of lysed cells into the cell culture medium. All tyrosine mutations resulted in reduced cytotoxic activity of Etx-H149A towards MDCK.2 cells [Fig. 5(A)], indicated by a right shift of the dose response curves relative to Etx-H149A. The dose of each toxin that killed 50% of the cells (CT_{50}) was determined by nonlinear regression analysis and the cytotoxic activity of each tyrosine mutant was expressed as the fold-change in CT_{50} relative to Etx-H149A. Mutants Y30A and Y196A showed significant reduction in cytotoxic activity toward MDCK.2 cells relative to Etx-H149A (27-fold and 10-fold increase in CT_{50}, respectively) [Fig. 5(B)].

Surface exposed tyrosine residues in domain I do not play a role in binding of P-Etx-H149A to ACHN cells

To determine whether surface exposed tyrosine residues in Domain I also play a role in binding of Etx to ACHN cells, we tested binding of the tyrosine mutants in H149A background to ACHN cells using the On-Cell Western assay. The binding activity of each tyrosine mutant was expressed as the fold-change in fluorescence intensity relative to P-Etx-H149A. ACHN cells treated with all of the tyrosine mutants showed fluorescence similar to that of cells treated with P-Etx-H149A (Fig. 6), indicating that surface exposed tyrosine residues in Domain I do not mediate binding of Etx to ACHN cells.

Next, we measured LDH release from ACHN cells exposed to mutants Y30A and Y196A, mutants

Table II. *The Reduced Binding Ability of the Tyrosine Mutants Correlates with Their Reduced Ability to Bind to MDCK.2 Cells*

Etx-H149A mutant	Mean fold-change in CT_{50} relative to Etx-H149A	Mean fold-change in fluorescence intensity relative to P-Etx-H149A
Y30A	27.8 ± 7.3***	−20.7 ± 4.5***
Y196A	9.1 ± 2.1**	−6.0 ± 2.6**
Y36A	5.7 ± 2.6	−3.7 ± 1.5
Y29A	4.1 ± 2.2	−3.3 ± 0.6
Y16A	3.5 ± 2.9	−1.7 ± 0.6
Y20A	2.5 ± 1.3	−1.3 ± 0.6

The binding activity of each Tyr mutant was expressed as the fold-change in fluorescence intensity relative to P-Etx-H149A as determined in Figure 4. The cytotoxic activity of tyrosine mutants was expressed as the fold-change in CT_{50} relative to Etx-H149A as determined in Figure 5(B). Statistically significant differences are indicated by asterisks.

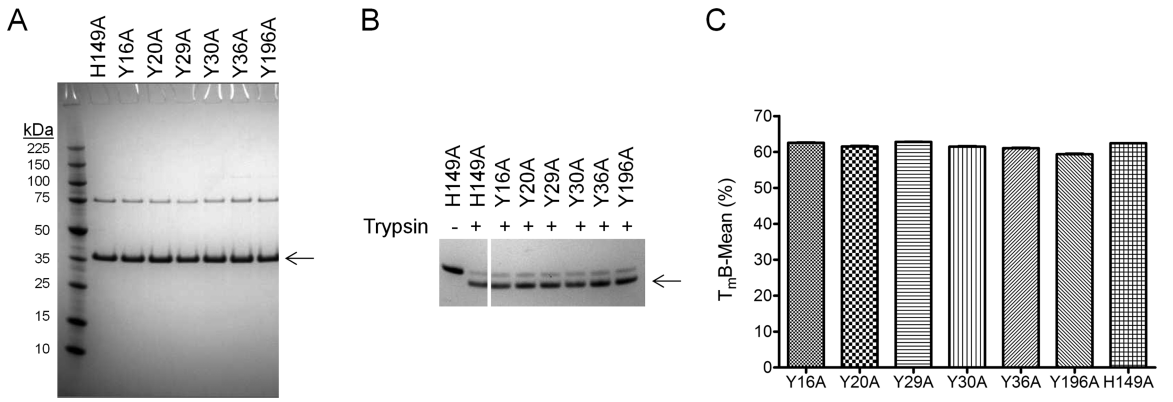

Figure 3. Recombinant tyrosine mutants in H149A background are folded correctly. Inactive prototoxins (A) and trypsin activated toxins (B) were separated by SDS-PAGE and visualized by Coomassie staining. Arrows indicate the positions of monomeric epsilon prototoxins and trypsin-activated toxins, respectively. (C) Thermo-stability of P-Etx-H149A and its derivatives were determined by the Boltzmann method using the Protein Thermal Shift software (Applied Biosystems).

that showed significantly reduced binding and cytotoxic activities toward MDCK.2 cells. The results of our cytotoxicity assay revealed that Etx-H149A and its derivatives are unable to cause cell lysis in ACHN cells, while wild-type Etx was able to cause approximately 45% cell lysis at the maximum dose of 10 μ*M* tested (Fig. 7).

Discussion

Epsilon toxin is a potent toxin and is classified as a category B bioterrorism agent,[30] making genetic modification of the toxin hazardous. In this study, we showed that the H149A mutation does not affect the overall organisation of the putative receptor binding loops in domain I. Residue H149 is located in Domain III of Etx in close proximity to the tip of the β-hairpin in Domain II. Therefore, the H149A mutation is likely to interfere with the conformation changes associated with insertion of the β-hairpin into the membrane and thus with membrane insertion of the toxin. It has previously been shown that creating disulphide bonds between pairs of introduced cysteines (one in the β-hairpin and one in an adjacent strand) prevented pore formation but not receptor binding or oligomerization of the toxin,[31] providing further support that interfering with pore formation of Etx does not affect its receptor binding.

Our cytotoxicity and binding data show that residues Y30 and Y196 play an important role in cell binding and thus, cytotoxicity of Etx toward MDCK.2 cells. All of the tyrosine mutants that we have cloned, expressed and purified in H149A background were soluble and stable, and our thermal stability analysis indicated that these proteins are correctly folded, ruling out the possibility that the reduced binding and cytotoxic activities of the tyrosine mutants towards MDCK.2 cells was due to their change in structure. The average CT_{50} for Etx-H149A towards MDCK.2 cells was 400 ng/mL (12 n*M*), in agreement with the reported CT_{50} of 20 to 300 ng/mL for the more active wild-type Etx.[22,23,25,32] We also showed that tyrosine mutants in H149A background mimic the behavior of tyrosine mutants in wild-type background,[16] confirming the role of domain I in binding of Etx to MDCK cells, and thus the suitability of the H149A mutant for further receptor binding studies.

The human kidney carcinoma cell line, ACHN, has recently been identified to be susceptible to Etx[26] but the role of surface exposed tyrosine residues in binding of Etx to this cell line has not been determined. Using the H149A mutant as a platform to study binding of tyrosine mutants to ACHN cells we showed that surface exposed tyrosine residues in domain I of Etx do not mediate binding of Etx to ACHN cells, suggesting that alternative amino acids within the toxin contribute to binding of Etx to these cells. The crystal structure of P-Etx-H149A also identified a glycan (β-octyl-glucoside) binding site in domain III of Etx-H149A, suggesting the presence of a secondary binding site in Etx in this region. Recent evidence also indicates the presence of a

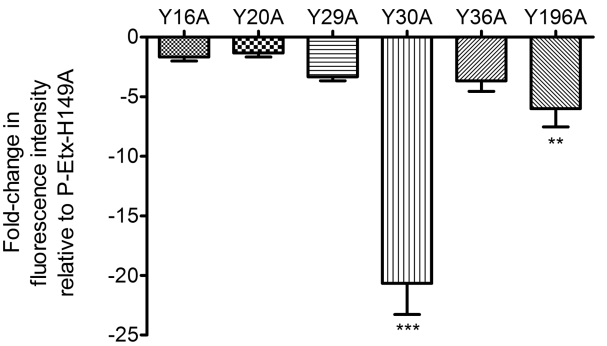

Figure 4. Effect of tyrosine substitutions on the binding of P-Etx-H149A to MDCK.2 cells. The binding of tyrosine mutants to MDCK.2 cells was determined by the On-Cell Western assay. Statistically significant differences between P-Etx-H149A and tyrosine mutant proteins are indicated by asterisks.

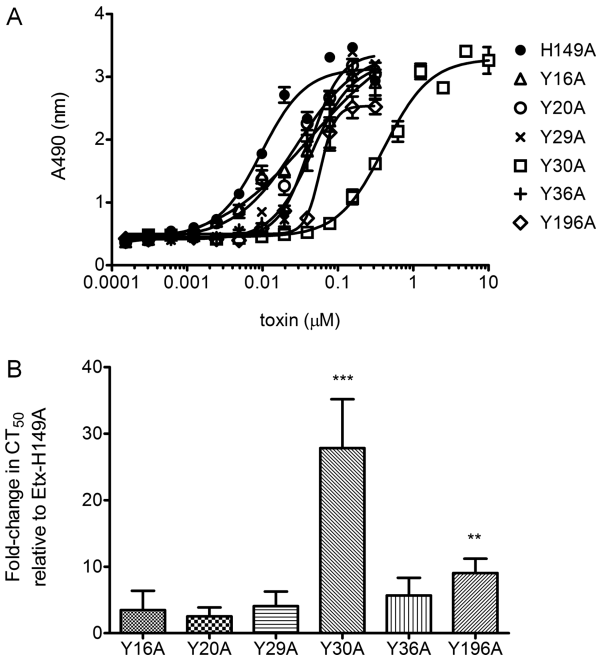

Figure 5. Effect of the tyrosine mutations on the cytotoxic activity of Etx-H149A toward MDCK.2 cells. (A) The cytotoxic activity of trypsin-activated toxins toward MDCK.2 cells was determined by measuring the release of lactate dehydrogenase (LDH) from lysed cells. (B) The dose of each toxin that killed 50% of the cells (CT_{50}) was determined and cytotoxic activity of tyrosine mutants was expressed as the fold-change in CT_{50} relative to Etx-H149A. Statistically significant differences between Etx-H149A and tyrosine mutant proteins are indicated by asterisks.

secondary binding site for lysenin, a sphingomyelin-specific pore-forming protein,[33] in a location similar to the β-OG binding site in Etx.

The results of our cytotoxicity assay also revealed that ACHN cells are more resistant to Etx induced cell lysis than MDCK.2 cells. Wild-type Etx in ACHN cells was only able to cause up to 45% cell lysis, even at the maximum dose of 10 μ*M* tested, while a dose of wild-type Etx approximately 10,000-fold less is able to cause 50% cell lysis in MDCK.2 cells,[22,23,25,32] suggesting that the mechanism of Etx-induced intoxication in ACHN and MDCK cells is different. Several lines of evidence suggest that Etx-induced cytotoxicity differs in different cell lines. In particular, Chassin *et al.*[23] reported that Etx-induced intracellular Ca^{2+} rise and ATP depletion-mediated rapid cell death in $mpkCCD_{cl14}$ cells occurred even under conditions that prevented toxin oligomerization and pore formation, providing evidence that pore formation is not the only way Etx manifests its cytotoxicity. The differences in the relative sensitivity of MDCK.2 and ACHN cells to Etx are likely to be due to the differences in the mode of action of Etx on these two cell lines, probably due to the ability of Etx to recognise different targets on the cell surface of different cells.

There is no evidence for a single receptor for epsilon toxin. Studies using MDCK cells suggest that binding of Etx is mediated by O-linked oligosaccharides as removal of O-glycans by β-elimination reduced binding of Etx to these cells.[34] Other studies implicated that interaction of Etx with target cells is mediated by the O-linked glycans of the extracellular domain of the human hepatitis A virus cellular receptor (HAVCR1).[16,26] Although disrupting expression of HAVCR1 in MDCK and ACHN cells led to increased resistance to Etx-induced cytotoxicity,[26] providing good evidence that both of these cell lines express HAVCR1, no direct evidence exists that the toxin binds to HAVCR1 on these cells. Furthermore, studies using synaptosomal fractions isolated from rat brain indicate that the receptor for Etx in the brain is a sialoglycoprotein.[35] In this study, we provide further indirect evidence that Etx binds to glycans by identifying a β-OG binding site in-between two β-sheets in domain III. In addition, a second unidentified ligand, likely to be β-OG, was found in the proximity of Y29 in domain I, providing further circumstantial evidence for the role of domain I in glycan binding.

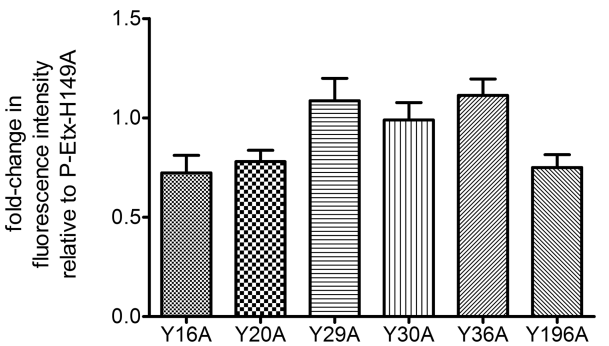

Figure 6. Effect of the tyrosine mutations on the binding of P-Etx-H149A to ACHN cells. The binding of tyrosine mutants to ACHN cells was determined by the On-Cell Western assay.

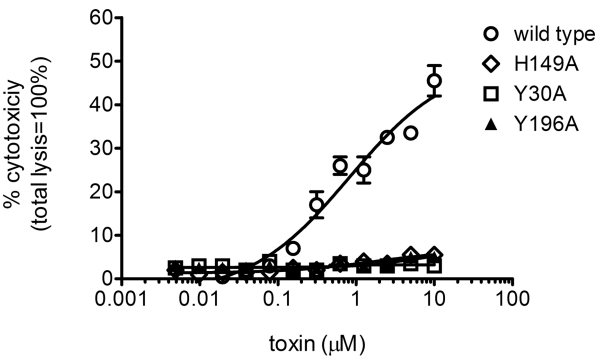

Figure 7. Effect of tyrosine substitutions on the cytotoxicity of Etx-H149A toward ACHN cells. The cytotoxic activity of trypsin-activated toxins towards ACHN cells was determined by measuring the release of LDH from lysed cells. Results were normalized to the signal from cells treated with PBS only (0% lysis) and cells treated with 0.9% (v/v) Triton X-100 (100% lysis).

In conclusion, the present study confirmed the role of surface exposed tyrosine residues in binding of Etx to MDCK.2 cells and demonstrated the suitability of the H149A mutant for further receptor binding studies. However, we found no evidence that surface exposed tyrosine residues in domain I mediate binding of Etx to ACHN cells, suggesting that Etx recognises different targets on the cell surface of different cells. These findings have important implications for developing strategies designed to neutralise the activity of this potent toxin.

Materials and Methods

Cell culture

MDCK.2 cells (ATCC-LGC Standards, Teddington, UK) and ACHN cells (ECACC, Salisbury, UK) were routinely cultured in Eagle's Minimum Essential Medium (EMEM; ATCC-LGC Standards, Teddington, UK) supplemented with 10% Foetal Bovine Serum Gold (PAA, Pasching, Austria) at 37°C in a humidified atmosphere of 95% air/5% CO_2. The culture medium was replaced every 2 to 3 days. Cells were routinely detached by incubation in trypsin/EDTA and split as appropriate (typically 1:6 dilutions).

Cloning of recombinant epsilon prototoxin P-Etx-H149A

The *etxD* gene encoding epsilon prototoxin with the H149A mutation (P-Etx-H149A) was subcloned from plasmid pCl0[28] into the expression vector pET-26b(+) (Merck, Darmstadt, Germany) using *Nco*I and *Xho*I restriction sites. This fused the N-terminal end of P-Etx-H149A without the 13 N-terminal residues (KEISNTVSNEMSK) to the PelB leader peptide, while the C-terminal end of P-Etx-H149A was fused to a polyhistidine (6 × His) affinity tag to aid purification of recombinant P-Etx-H149A (Fig. 2). The recombinant plasmid expressing P-Etx-H149A is termed pET26-b(+)/P-Etx-H149A. All amino acid numbering corresponds to prototoxin with the 13 amino acids N-terminal peptide sequence removed, unless otherwise stated.

Site-directed mutagenesis

Mutations were introduced into the gene encoding P-Etx-H149A using the QuickChange Lightning Site-Directed Mutagenesis Kit (Agilent Technologies, Inc., Santa Clara) according to the manufacturer's instructions. Synthetic oligonucleotide primer pairs (Eurofins MWG Operon, Ebersberg, Germany) were used to change each tyrosine codon to an alanine codon. To create Tyr mutants, plasmid pET26-b(+)/P-Etx-H149A served as template. The presence of the intended mutations was verified by DNA sequencing (Source BioScience, Cambridge, UK).

Expression and purification of P-Etx-H149A and its derivatives

For expression of P-Etx-H149A and its derivatives, recombinant plasmids were transferred into *E. coli* Rosetta 2 (DE3) cells (Merck, Darmstadt, Germany) and expression of P-Etx-H149A and its derivatives was induced using the autoinduction system as described by Studier.[28] In brief, cells (100 mL) were grown in ZYM-5052 autoinducing medium supplemented with 50 μg/mL kanamycin and 34 μg/mL chloramphenicol and cultured at 37°C for 3 h at 300 rpm, then for a further 24 h at 20°C, 300 rpm.

For protein purification, cells were harvested by centrifugation and 2 g of cell pellet was lysed by 10 mL BugBuster™ Protein Extraction Reagent (Merck, Darmstadt, Germany) containing 10 μL rlysozyme™ (1 KU/μL) (Merck, Darmstadt, Germany) and 10 μL Benzonase® Nuclease (25 U/μL) (Merck, Darmstadt, Germany). The cell suspension was incubated on a rotating mixer for 25 min at room temperature and centrifuged at 16,000*g* for 20 min at 4°C to separate soluble and insoluble fractions. The supernatant was loaded onto a His GraviTrap column (GE Healthcare Life Sciences, Little Chalfont, UK) following the manufacturer's guidelines. In brief, His-tagged proteins were bound to the affinity column using a buffer composed of 20 m*M* sodium phosphate, 500 m*M* NaCl, 20 m*M* imidazole, pH 7.4. The column was washed with a buffer composed of 20 m*M* sodium phosphate, 500 m*M* NaCl, 60 m*M* imidazole, pH 7.4. Recombinant prototoxin was eluted in a buffer composed of 20 m*M* sodium phosphate, 500 m*M* NaCl, 500 m*M* imidazole, pH 7.4. All purification steps were carried out at 4°C. For buffer exchange and sample clean up, prototoxin containing eluate was applied to a PD-10 Desalting Column (GE Healthcare Life Sciences, Little Chalfont, UK) and eluted in 10 m*M* phosphate buffer, 2.7 m*M* potassium chloride, 137 m*M* NaCl, pH 7.4. Protein concentrations were determined using the BCA assay (Fisher Scientific UK Ltd, Loughborough, UK).

The purity of P-Etx-H149A and its derivatives was confirmed by SDS-PAGE. Proteins were resolved by 4 to 12% Bis-Tris NuPAGE gels (Invitrogen Ltd., Paisley, UK) using Surelock Xcell apparatus (Invitrogen Ltd., Paisley, UK) and NuPAGE MES SDS running buffer (Invitrogen Ltd., Paisley, UK). All samples were heated before loading at 70°C for 10 min in NuPAGE LDS sample buffer (Invitrogen Ltd., Paisley, UK). Gels were run at 200 V for 45 min. After electrophoretic separation, proteins were visualised by SimplyBlue staining (Invitrogen Ltd., Paisley, UK). The Perfect Protein™ Marker, 10 to 225 kDa (Merck, Darmstadt, Germany) was used as the molecular weight standard.

Crystallization and data processing

For crystallization experiments a modified construct of P-Etx-H149A was used with a TEV cleavable N-terminal His-tag and a Factor Xa cleavage (IEGR) site engineered in between amino acids K260 and

K261, which allows potential activation of P-Etx-H149A by Factor Xa. Purification of P-Etx-H149A was carried out using standard metal affinity chromatography followed by removal of the N-terminal His-tag by TEV protease. A final size exclusion chromatography step was performed using a 120 mL Superdex S-200 column equilibrated with 20 m*M* Tris pH 7.5, 150 m*M* NaCl, and 1 m*M* DTT. Recombinant P-Etx-H149A was concentrated to 16 mg/mL using a 10 kDa cut-off Amicon concentrator (Merck, Darmstadt, Germany). Crystals were obtained using the hanging drop method in 0.85 *M* ammonium dihydrogen phosphate and 0.5% (w/v) β-octyl-glucoside (β-OG). Data were collected on a Rigaku Saturn 944 CCD detector mounted onto a Rigaku Micromax X-ray generator. Data were indexed and integrated and scaled with D*TREK.[36] Molecular replacement was carried out using Phaser MR[37] as part of the CCP4 package[38] using the wild-type structure (PDB ID: 1UYJ) as a search model. Refinement was carried out using Refmac 5,[39] and manual building and real space refinement was performed using COOT.[40] Model validation was calculated using Molprobity[41] and PyMOL[42] was used for visualisation and figure preparation.

Activation of P-Etx-H149A and its derivatives by trypsin

Purified recombinant P-Etx-H149A and its derivatives were activated with trypsin, TPCK treated from bovine pancreas (Sigma-Aldrich Company Ltd., Gillingham, UK), which removes the C-terminal peptide sequence, together with the His-tag (Fig. 1). Trypsin was prepared in PBS and added to recombinant prototoxin at 1:100 (w/w) ratio and incubated at room temperature for 1 h. Protease Inhibitor Cocktail, EDTA-Free (Fisher Scientific UK Ltd, Loughborough, UK) was added to the digest to inhibit trypsin in the samples. Removal of the C-terminal peptide sequence was assessed by SDS-PAGE.

Protein thermal shift assay

Thermostability of P-Etx-H149A and its derivatives was assessed by mixing purified recombinant prototoxin (0.25 mg/mL) with 240× SYPRO Orange dye (Sigma) in triplicate and fluorescence was monitored using a StepOnePlus quantitative PCR machine (Applied Biosystems) with a 1% thermal gradient from 25°C to 99°C. Fluorescence data was analysed by the Protein Thermal Shift Software (Applied Biosystems) to calculate the T_m using the Boltzmann method.

Cytotoxicity assay

The cytotoxic activity of trypsin-activated Etx-H149A and its derivatives toward MDCK.2 and ACHN cells was determined by measuring the amount of lactate dehydrogenase (LDH) released from the cytosol of lysed cells into the cell culture medium using the CytoTox 96 nonradioactive cytotoxicity assay kit (Promega, Southampton, UK) according to the manufacturer's protocol. In brief, a twofold dilution series of each activated toxin (ranging from 10 μ*M* to 0.15 n*M*) was prepared in PBS and added to cells seeded into 96-well plates (3×10^4 cells/well). Following incubation at 37°C for 3 h, cell culture medium (50 μL) was harvested from cell monolayers, transferred to a fresh 96-well enzymatic assay plate and 50 μL of reconstituted substrate mix was added to each well. The plate was incubated for 30 min at room temperature, protected from light. Absorbance was measured at 490 nm using a Model 680 Microplate Reader (Bio-Rad Laboratories Ltd., Hemel Hempstead, UK). The absorbance values for each sample were normalized by subtracting the absorbance value obtained for the culture medium from untreated cells. The toxin dose required to kill 50% of the cell monolayer (CT_{50}) was determined by nonlinear regression analysis, fitting a variable slope log(dose) versus response curve, constraining *F* to a value of 50 ($\log CT_{50} = \log CTF - (1/\text{HillSlope}) \times \log(F/(100 - F))$).

On-Cell Western assay

On-Cell Western assay was used to measure binding of P-Etx-H149A and its derivatives to MDCK.2 and ACHN cells. Black 96-well microtiter plates were seeded with 3×10^4 cells/well in EMEM medium containing 10% foetal bovine serum. To allow cells to attach, plates were incubated overnight at 37°C in a humidified atmosphere of 95% air/5% CO2. The next day, plates were washed with PBS and cells were incubated with purified recombinant prototoxin (10 μ*M*) for 1 h at 37°C in a humidified atmosphere of 95% air/5% CO2. For background control, triplicate wells were incubated with PBS only. Unbound toxin was removed by washing cell monolayers three times with PBS. Cells were then fixed with 4% formaldehyde at room temperature for 20 min. After washing the cell monolayers with PBS three times, cells were blocked for 1.5 h using Odyssey blocking buffer (LI-COR Biosciences, Lincoln, NE). Bound prototoxin was detected with mouse anti-His Tag monoclonal antibody (Invitrogen Ltd., Paisley, UK) and IRDye 800CW goat anti-mouse IgG (H + L) antibody (LI-COR Biosciences, Lincoln) at 1:500 dilution each. Plates were imaged at 800 nm using the Odyssey CLx infrared imaging system (LI-COR Biosciences, Lincoln) to quantify the amount of fluorescent signal. The fluorescent signal from wells treated with prototoxin was normalized to that of wells treated with PBS only and the binding activity of each tyrosine mutant was expressed as the fold-change in fluorescence intensity relative to P-Etx-H149A.

Statistical analysis

To compare the means of protein thermal shift, On-Cell Western and cytotoxicity data, one-way ANOVA analysis followed by Dunnett's post test (***$P < 0.001$, **$P < 0.01$) was carried out using the GraphPad Prism software 5.01 (GraphPad Software, La Jolla). In all analyses, a P value of less than 0.01 was considered significant. All data represent the means and standard deviations of three independent experiments performed in triplicate.

Accession numbers

The structure coordinates of P-Etx-H149A have been deposited at the Protein Data Bank (http://www.pdb.org), PDB ID: 3ZJX. Amino acid numbering corresponds to prototoxin with the 13 amino acids N-terminal peptide sequence.

Acknowledgments

The authors thank Michel R. Popoff, Institut Pasteur, for providing wild-type epsilon toxin and Nick Harmer, University of Exeter for helpful discussions and commenting on the article.

References

1. Bokori-Brown M, Savva CG, Fernandes da Costa SP, Naylor CE, Basak AK, Titball RW (2011) Molecular basis of toxicity of *Clostridium perfringens* epsilon toxin. FEBS J 278:4589–4601.
2. Uzal FA, Songer JG (2008) Diagnosis of *Clostridium perfringens* intestinal infections in sheep and goats. J Vet Diagn Invest 20:253–265.
3. Songer JG (1996) Clostridial enteric diseases of domestic animals. Clin Microbiol Rev 9:216–234.
4. Popoff MR (2011) Epsilon toxin: a fascinating pore-forming toxin. FEBS J 278:4602–4615.
5. Nagahama M, Sakurai J (1993) Effect of drugs acting on the central nervous system on the lethality in mice of *Clostridium perfringens* epsilon toxin. Toxicon 31: 427–435.
6. Miyamoto O, Minami J, Toyoshima T, Nakamura T, Masada T, Nagao S, Negi T, Itano T, Okabe A (1998) Neurotoxicity of *Clostridium perfringens* epsilon-toxin for the rat hippocampus via the glutamatergic system. Infect Immun 66:2501–2508.
7. Miyamoto O, Sumitani K, Nakamura T, Yamagami S, Miyata S, Itano T, Negi T, Okabe A (2000) *Clostridium perfringens* epsilon toxin causes excessive release of glutamate in the mouse hippocampus. FEMS Microbiol Lett 189:109–113.
8. Lonchamp E, Dupont JL, Wioland L, Courjaret R, Mbebi-Liegeois C, Jover E, Doussau F, Popoff MR, Bossu JL, de Barry J, Poulain B (2010) *Clostridium perfringens* epsilon toxin targets granule cells in the mouse cerebellum and stimulates glutamate release. PLoS One 5:e13046.
9. Finnie JW (2003) Pathogenesis of brain damage produced in sheep by *Clostridium perfringens* type D epsilon toxin: a review. Aust Vet J 81:219–221.
10. Popoff MR, Bouvet P (2009) Clostridial toxins. Future Microbiol 4:1021–1064.
11. McDonel JL, Toxins of *Clostridium perfringens* types A, B, C, D and E. In: Dorner F, Drews J, Eds. (1986) Pharmacology of bacterial toxins. Oxford: Pergamon Press, pp 477–517.
12. Bhown AS, Habeerb AF (1977) Structural studies on epsilon-prototoxin of *Clostridium perfringens* type D. Localization of the site of tryptic scission necessary for activation to epsilon-toxin. Biochem Biophys Res Commun 78:889–896.
13. Jin F, Matsushita O, Katayama S, Jin S, Matsushita C, Minami J, Okabe A (1996) Purification, characterization, and primary structure of *Clostridium perfringens* lambda-toxin, a thermolysin-like metalloprotease. Infect Immun 64:230–237.
14. Minami J, Katayama S, Matsushita O, Matsushita C, Okabe A (1997) Lambda-toxin of *Clostridium perfringens* activates the precursor of epsilon-toxin by releasing its N- and C-terminal peptides. Microbiol Immunol 41:527–535.
15. Cole AR, Gibert M, Popoff M, Moss DS, Titball RW, Basak AK (2004) *Clostridium perfringens* epsilon-toxin shows structural similarity to the pore-forming toxin aerolysin. Nat Struct Mol Biol 11:797–798.
16. Ivie SE, McClain MS (2012) Identification of amino acids important for binding of *Clostridium perfringens* epsilon toxin to host cells and to HAVCR1. Biochemistry 51:7588−7595.
17. Parker MW, Buckley JT, Postma JP, Tucker AD, Leonard K, Pattus F, Tsernoglou D (1994) Structure of the *Aeromonas* toxin proaerolysin in its water-soluble and membrane-channel states. Nature 367:292–295.
18. Miyata S, Minami J, Tamai E, Matsushita O, Shimamoto S, Okabe A (2002) *Clostridium perfringens* epsilon-toxin forms a heptameric pore within the detergent-insoluble microdomains of MDCK cells and rat synaptosomes. J Biol Chem 277:39463–39468.
19. Abrami L, van Der Goot FG (1999) Plasma membrane microdomains act as concentration platforms to facilitate intoxication by aerolysin. J Cell Biol 147:175–184.
20. Abe Y, Shimada H, Kitada S (2008) Raft-targeting and oligomerization of Parasporin-2, a *Bacillus thuringiensis* crystal protein with anti-tumour activity. J Biochem 143:269–275.
21. Nagahama M, Ochi S, Sakurai J (1998) Assembly of *Clostridium perfringens* epsilon-toxin on MDCK cell membrane. J Nat Toxins 7:291–302.
22. Petit L, Gibert M, Gillet D, Laurent-Winter C, Boquet P, Popoff MR (1997) *Clostridium perfringens* epsilon-toxin acts on MDCK cells by forming a large membrane complex. J Bacteriol 179:6480–6487.
23. Chassin C, Bens M, de Barry J, Courjaret R, Bossu JL, Cluzeaud F, Ben Mkaddem S, Gibert M, Poulain B, Popoff MR, Vandewalle A (2007) Pore-forming epsilon toxin causes membrane permeabilization and rapid ATP depletion-mediated cell death in renal collecting duct cells. Am J Physiol Renal Physiol 293:F927–F937.
24. Knight PA, Queminet J, Blanchard JH, Tilleray JH (1990) In vitro tests for the measurement of clostridial toxins, toxoids and antisera. II. Titration of *Clostridium perfringens* toxins and antitoxins in cell culture. Biologicals 18:263–270.
25. Payne DW, Williamson ED, Havard H, Modi N, Brown J (1994) Evaluation of a new cytotoxicity assay for *Clostridium perfringens* type D epsilon toxin. FEMS Microbiol Lett 116:161–167.
26. Ivie SE, Fennessey CM, Sheng J, Rubin DH, McClain MS (2011) Gene-trap mutagenesis identifies mammalian genes contributing to intoxication by *Clostridium perfringens* epsilon-toxin. PLoS One 6:e17787.
27. Recommendations of the CDC Strategic Planning Workgroup (2000) Biological and chemical terrorism:

strategic plan for preparedness and response. MMWR Recomm Rep 49:1–14.
28. Oyston PCF, Payne DW, Havard HL, Williamson ED, Titball RW (1998) Production of a non-toxic site-directed mutant of *Clostridium perfringens* epsilon-toxin which induces protective immunity in mice. Microbiology 144:333–341.
29. Lavinder JJ, Hari SB, Sullivan BJ, Magliery TJ (2009) High-throughput thermal scanning: a general, rapid dye-binding thermal shift screen for protein engineering. J Am Chem Soc 131:3794–3795.
30. Diep DB, Nelson KL, Lawrence TS, Sellman BR, Tweten RK, Buckley JT (1999) Expression and properties of an aerolysin - *Clostridium septicum* alpha toxin hybrid protein. Mol Microbiol 31:785–794.
31. Pelish TM, McClain MS (2009) Dominant-negative inhibitors of the *Clostridium perfringens* epsilon-toxin. J Biol Chem 284:29446–29453.
32. McClain MS, Cover TL (2007) Functional analysis of neutralizing antibodies against *Clostridium perfringens* epsilon-toxin. Infect Immun 75:1785–1793.
33. De Colibus L, Sonnen AF, Morris KJ, Siebert CA, Abrusci P, Plitzko J, Hodnik V, Leippe M, Volpi E, Anderluh G, Gilbert RJ (2012) Structures of lysenin reveal a shared evolutionary origin for pore-forming proteins and its mode of sphingomyelin recognition. Structure 20:1498–1507.
34. Dorca-Arevalo J, Martin-Satue M, Blasi J (2012) Characterization of the high affinity binding of epsilon toxin from *Clostridium perfringens* to the renal system. Vet Microbiol 157:179–189.
35. Nagahama M, Sakurai J (1992) High-affinity binding of *Clostridium perfringens* epsilon-toxin to rat brain. Infect Immun 60:1237–1240.
36. Pflugrath JW (1999) The finer things in X-ray diffraction data collection. Acta Crystallogr D Biol Crystallogr 55:1718–1725.
37. McCoy AJ, Grosse-Kunstleve RW, Adams PD, Winn MD, Storoni LC, Read RJ (2007) Phaser crystallographic software. J Appl Crystallogr 41:658–674.
38. Winn MD, Ballard CC, Cowtan KD, Dodson EJ, Emsley P, Evans PR, Keegan RM, Krissinel EB, Leslie AG, McCoy A, McNicholas SJ, Murshudov GN, Pannu NS, Potterton EA, Powell HR, Read RJ, Vagin A, Wilson KS (2011) Overview of the CCP4 suite and current developments. Acta Crystallogr D Biol Crystallogr 67: 235–242.
39. Murshudov GN, Vagin AA, Dodson EJ (1997) Refinement of macromolecular structures by the maximum-likelihood method. Acta Cryst D53:240–255.
40. Emsley P, Lohkamp B, Scott WG, Cowtan K (2010) Features and development of Coot. Acta Cryst D Biol Crystallogr 66:486–501.
41. Davis IW, Leaver-Fay A, Chen VB, Block JN, Kapral GJ, Wang X, Murray LW, Arendall WB, 3rd, Snoeyink J, Richardson JS, Richardson DC (2007) MolProbity: all-atom contacts and structure validation for proteins and nucleic acids. Nucleic Acids Res 35: W375–383.
42. The PyMOL Molecular Graphics System, Version 1.3r1 (2010) Schrödinger LLC. http://www.pymol.org/citing.